Robust magnetic polarons in type-II (Zn,Mn)Te/ZnSe magnetic quantum dots

I. R. Sellers,[1,*,†] R. Oszwałdowski,[1,2,‡] V. R. Whiteside,[1] M. Eginligil,[1] A. Petrou,[1] I. Zutic,[1] W.-C. Chou,[3] W. C. Fan,[3] A. G. Petukhov,[4] S. J. Kim,[5] A. N. Cartwright,[5] and B. D. McCombe[1]

[1]*Department of Physics, University at Buffalo–SUNY, Buffalo, New York 14260, USA*

[2]*Instytut Fizyki, Uniwersytet M. Kopernika, Grudziądzka 5/7, Toruń 87-100, Poland*

[3]*Department of Electro-physics, National Chiao Tung University, Hsinchu 300, Taiwan*

[4]*Department of Physics, South Dakota School of Mines & Technology, Rapid City, South Dakota 57701, USA*

[5]*Department of Electrical & Electronic Engineering, University at Buffalo–SUNY, Buffalo, New York 14260, USA*

(Received 18 July 2010; revised manuscript received 28 October 2010; published 18 November 2010)

We present a magneto-optical study of magnetic polarons in type-II (Zn,Mn) Te quantum dots. The polarons are formed due to the exchange coupling between the spins of the holes and those of the Mn ions, both of which are localized in the dots. In our photoluminescence studies, the magnetic polarons are detected at temperatures up to ~150 K, with a formation energy of ~40 meV. The emission from these dots exhibits an unusually small Zeeman shift with applied magnetic field (~2 meV at 8 T) and at the same time a very large circular polarization. We attribute this apparently contradictory behavior by a low and weakly temperature-dependent magnetic susceptibility due to antiferromagnetic coupling of the Mn spins.

DOI: 10.1103/PhysRevB.82.195320 PACS number(s): 78.55.Et, 71.35.Ji, 78.67.Hc, 85.35.Be

I. INTRODUCTION

The exchange interactions between the spins of magnetic ions and the spins of carriers in magnetic semiconductors lead to a variety of exotic magnetic effects.[1] Doping quantum dots (QDs) with magnetic ions such as Mn (Refs. 2–7) provides opportunities to study new magnetic effects not present in bulk magnetic semiconductors[1,8] and quantum wells (QWs).[9]

For example, adding an extra carrier in a QD can strongly modify both the total carrier spin and the onset temperature for magnetic order.[10–12] By controlling the quantum confinement in a QD, it is possible to create or destroy magnetic order, even at a fixed number of carriers.[13] One of the methods used to study the properties of magnetic QDs is photoluminescence (PL) spectroscopy, which provides a sensitive probe of the magnetic properties of these zero-dimensional systems. For example, PL spectroscopy has been used to study the shape of quantum confinement and the placement of Mn ions in CdTe QDs.[4] The exchange interaction between the spin of the Mn ions and the spin of a carrier leads to the formation of bound magnetic polarons (BMPs) in bulk semiconductors.[1,14–16] A BMP consists of a carrier bound on an impurity, with the carrier spin coupled to the spins of the magnetic ions within the Bohr radius of the impurity. In QWs, magnetic polarons are formed when carriers are localized on well-width fluctuations.[9,17] More recently, MPs have been studied in QDs,[2,7,18] where the confinement plays the role of the potential generated by the impurity in bulk material or the well-width fluctuations in QWs. The tunability of the QD confinement, which is absent in BMPs, makes the MPs in quantum dots a more versatile system.

During the formation of MPs in QDs, the exchange interaction between the confined carrier and the magnetic ions aligns the Mn spins with the spin of the carrier, which leads to a reduction in the total energy of the carrier-Mn system. This results in a redshift of the interband transition energy as function of time, which is observable in time-resolved (TR) PL experiments.[2,7,18]

In this work, we report the results of a magneto-optical study of (Zn,Mn)Te/ZnSe QDs, characterized by a type-II band alignment, shown schematically in Fig. 1(a). The holes in this system are strongly confined in the (Zn,Mn)Te QDs by the large valence band offset while the electrons, forced to remain in the surrounding ZnSe matrix by the conduction band offset, are bound to the holes by Coulomb attraction.[19,20]

The strong spatial separation between electrons and holes increases the radiative lifetime by as much as two orders of

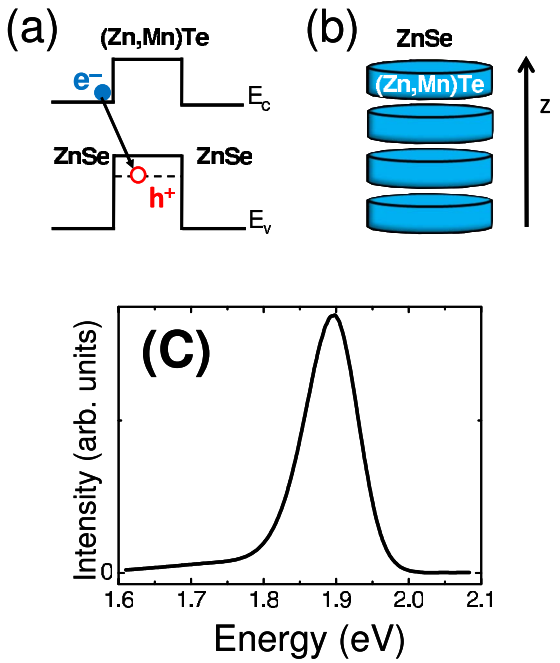

FIG. 1. (Color online) (a) Type-II band alignment in the (Zn,Mn)Te/ZnSe QD system. E_c and E_v are the conduction- and valence-band profiles, respectively. (b) The columnar geometry of the quantum dots. (c) Zero magnetic field photoluminescence at 4.2 K. Continuous-wave linearly polarized excitation is at 2.41 eV.

magnitude[21] with respect to type-I QDs.[22,23] The long lifetime of the type-II excitons facilitates the formation of robust MPs, as compared to type-I magnetic QDs, where the formation is limited by higher recombination rates.[2] Furthermore, in type-I magnetic QDs, for which the majority of prior experiments[2–6] have been performed, the interband transitions compete with the Mn internal transition at $E_{int} \sim 2.2$ eV,[1] when the band gap, E_g, exceeds E_{int}. In the (Zn,Mn)Te/ZnSe system investigated here, this competition is absent due to the type-II band alignment, since the indirect band gap $E_g < E_{int}$, in spite of the fact that both the ZnSe and (Zn,Mn)Te direct band gaps are larger than E_{int}. To avoid the energy transfer to the Mn transitions, in the previously studied CdSe/(Zn,Mn)Se type-I system, the nonmagnetic CdSe dots were grown embedded in a (Zn,Mn)Se magnetic barrier matrix.[2] The exchange interaction in those QDs, which confine both electrons and holes, is determined mostly by the limited penetration of the carrier wave function into the magnetic barriers. In contrast, in the (Zn,Mn)Te/ZnSe structures studied here, the Mn ions are incorporated *within* the QDs, resulting in a greatly increased overlap of the hole and Mn wave functions, which leads to a significant enhancement in the exchange interactions. We refer mostly to the hole-Mn (h-Mn) exchange interaction because it is significantly stronger than the electron-Mn interaction.[1]

II. EXPERIMENTAL

We have used two samples in this study: sample 1 incorporates magnetic (Zn,Mn)Te QDs, while sample 2 has nonmagnetic ZnTe QDs, which is used as a reference. Both samples were grown by molecular-beam epitaxy on a (100) GaAs substrate. Following the deposition of a ZnSe buffer layer, five layers of (Zn,Mn)Te QDs were grown in the case of sample 1 (ZnTe QDs for sample 2) by migration enhanced epitaxy. In sample 1, the average Mn composition of the (Zn,Mn)Te QD layers is 5.2% as measured by energy dispersive x-ray spectroscopy. The QD layers in both samples were separated by 5 nm ZnSe spacer layers, and the structures were capped with a 50 nm ZnSe layer. Cross-sectional transmission electron microscopy images indicate that the QDs form columns along the growth direction as shown schematically in Fig. 1(b). This direction is taken to be the z axis. The full details of sample growth and optimization were given in Ref. 24. The samples were placed in an optical closed cycle refrigerator for work at zero magnetic field and in an optical magnet cryostat for magneto-optical studies. The latter were carried out in the Faraday geometry in which the emitted light propagation direction is parallel to the magnetic field applied along the z axis. The continuous wave (cw) PL was excited by the linearly polarized 514.5 nm (2. 41 eV) line of an argon-ion laser. The photoluminescence was analyzed by a single monochromator equipped with a charge coupled device multichannel detector. A combination of quarter-wave plate and linear analyzer was placed before the spectrometer entrance slit to separate the $\sigma+$ and $\sigma-$ components of the emission. The TR PL was excited using a pulsed laser system which emits linearly polarized light at a wavelength of 400 nm (repetition rate=250 kHz, pulse duration ~300 fs). The TR PL was spectrally resolved by a monochromator, and temporally analyzed by a streak camera (temporal resolution=40 ps).

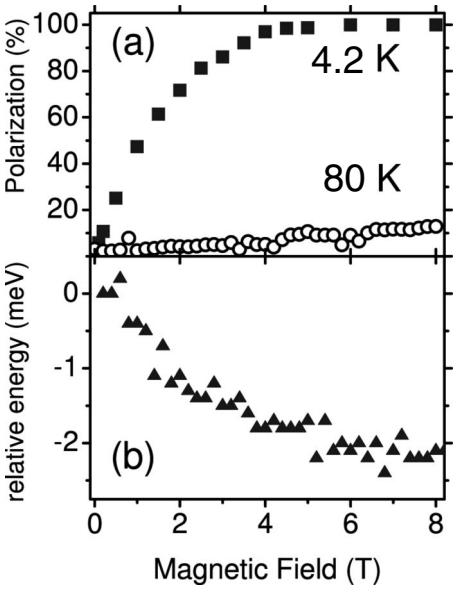

FIG. 2. (a) Circular polarization of the cw PL at 4.2 K and 80 K (squares) and 80 K (circles) plotted as function of applied magnetic field. (b) Shift of the PL peak energy with the magnetic field at T =4.2 K.

III. RESULTS AND DISCUSSION

In Fig. 1(c) we show the cw PL spectrum of sample 1 at temperature T=4.2 K and magnetic field B=0. The PL is excited nonresonantly by the 2.41 eV line of an argon-ion laser above the bulk (Zn,Mn)Te band gap (~2.39 eV) and below the ZnSe gap (~2.82 eV). The emission spectrum exhibits a peak at ~1.9 eV and is attributed to excitonic recombination across the interface between the (Zn,Mn)Te dots and the ZnSe matrix. The energy of the type-II interband transition is well below the energy of the Mn internal transition (~2.2 eV), and consequently the PL intensity of the former is much stronger than that of the latter.

Both (II,Mn)VI bulk materials[25] and QDs based on them[7,26] display giant excitonic Zeeman splittings (50–100 meV) even at moderate magnetic fields, which rapidly decrease with increasing temperature.[1] The dependence of the circular polarization of the excitonic emission from sample 1 on B is shown in Fig. 2(a) for T=4.2 and 80 K. At T=4.2 K the polarization increases monotonically with magnetic field and saturates at 95% for $B > 4$ T. The saturation polarization drops sharply with increasing temperatures and at T=80 K the polarization practically disappears.

This behavior is typical for magnetic (II,Mn)VI QDs, and is consistent with excitonic Zeeman splitting ΔE increasing with B and decreasing with T.[7,26] In Fig. 2(b) we plot the energy of the emission peak from sample 1 as function of magnetic field at T=4.2 K. At $B \sim 8$ T the energy shift in the PL peak (corresponding to $\Delta E/2$) is equal to only 2 meV. Unexpectedly the Zeeman splitting in sample 1 is an order of

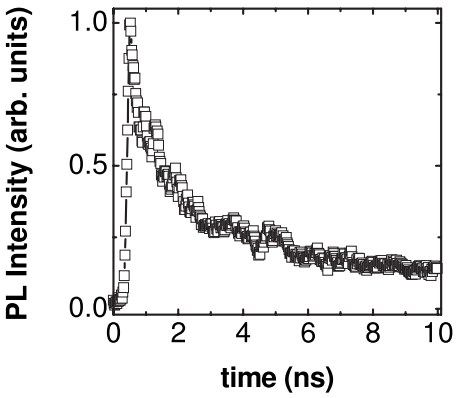

FIG. 3. PL intensity from sample 1 plotted as function of time delay after laser excitation; $T=14$ K.

magnitude smaller than the splitting observed in (Zn,Mn)Te bulk crystals,[25] as well as in magnetic QDs (Refs. 7 and 26) for comparable Mn compositions.

To explore how the unusually small Zeeman splitting can be compatible with the formation of magnetic polarons observed in type-I magnetic QDs, we have investigated the time evolution of the PL spectra at $B=0$. In Fig. 3, we plot the intensity of the PL as function of time delay from the laser pulse. The slow PL decay (recombination lifetime $\tau_R \sim 4$ ns) in this type-II QD system should allow for uninterrupted MP formation.

Figure 4 shows the normalized TR PL spectra in increments of 1.2 ns. Initially, the PL peak energy is ~1.924 eV, reaching a value of ~1.894 eV after a few nanosecond. Following Refs. 2 and 18, we attribute this evolution of the PL peak to the formation of MPs. In this process, the hole spin aligns the randomly oriented Mn spins, resulting in a Zeeman splitting[14] of the hole levels. In the low (high)-energy state of the MP, the Mn and hole spins are antiparallel (parallel). The TR PL peak position at $t=0$ corresponds to the exciton recombination energy prior to the alignment of the Mn spins. During the subsequent alignment, the hole occupies preferentially the lower Zeeman level and therefore the exciton PL peak undergoes a redshift as a function of time with a characteristic MP formation time τ_{MP}. In addition, during this process the linewidth of the PL narrows slightly (see Fig. 4), suggesting a reduction in the magnetic disorder of the QDs.[27]

The possibility of spurious effects such as the formation of a dipolar layer[28] was addressed by carrying out time-resolved PL measurements on the nonmagnetic ZnTe/ZnSe reference QD structure (sample 2). In Fig. 5, we show the evolution of the relative recombination energy for sample 1 and sample 2. Contrary to the behavior of sample 1, the PL energy of the nonmagnetic sample 2 remains constant within the formation time of MPs in sample 1. The comparison between the two samples verifies that the redshift in sample 1 has at its origin the magnetic properties of the dots and the formation of MPs, rather than band bending due to dipole layer formation.

In Fig. 6(a), we plot the PL peak energy from sample 1 as a function of time delay at various temperatures. The redshift which indicates the MP formation is observed up to 150 K;

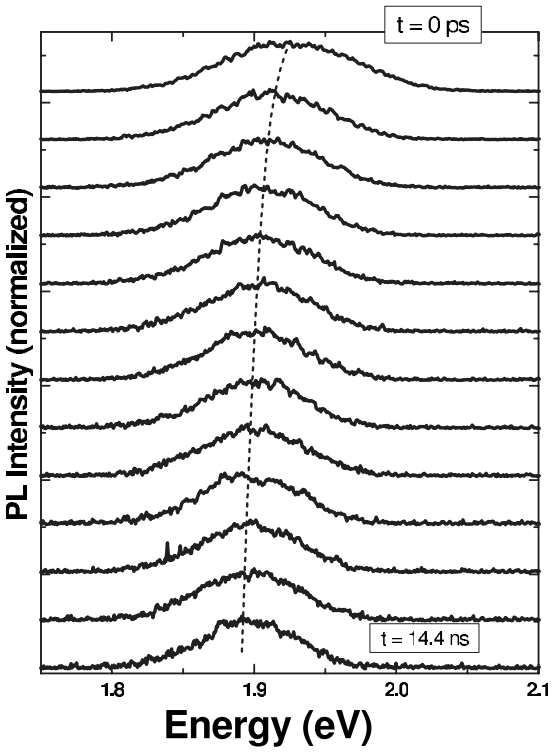

FIG. 4. Temporal evolution of the PL at 14 K in 1.2 ns steps. The PL peak intensities are normalized to the maximum intensity at time $t=0$.

we note that the MP in (Zn,Mn)Se/CdSe QDs persist only up to 30 K (Ref. 2) while in (Cd,Mn)Te QDs excited resonantly with circularly polarized light, the MP persists up to 120 K.[3]

To determine the MP binding energy, E_{MP}, and the formation time, τ_{MP}, at different temperatures, we fit the temporal evolution of the PL intensity peak energy in sample 1 by a double-exponential decay, rather than the single exponent used by other groups.[2,29,30] The fitted energy E_{MP} is plotted as function of temperature in Fig. 6(b). As can be seen, E_{MP} exhibits a surprisingly weak temperature dependence with an average value of 40 ± 1 meV. Using the fits to the data of Fig. 6(a), we find two separate timescales for all tempera-

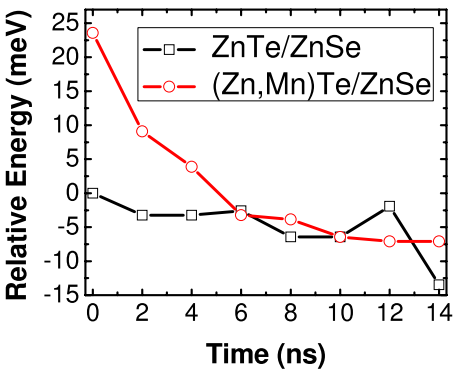

FIG. 5. (Color online) Comparison of the temporal evolution of the relative energy of the PL peak for the magnetic Zn(Mn,Te)/ZnSe sample 1 (circles) and nonmagnetic ZnTe/ZnSe sample 2 (squares) at 14 K. The zero of the energy axis corresponds to the emission peak energy of the nonmagnetic sample at $t=0$.

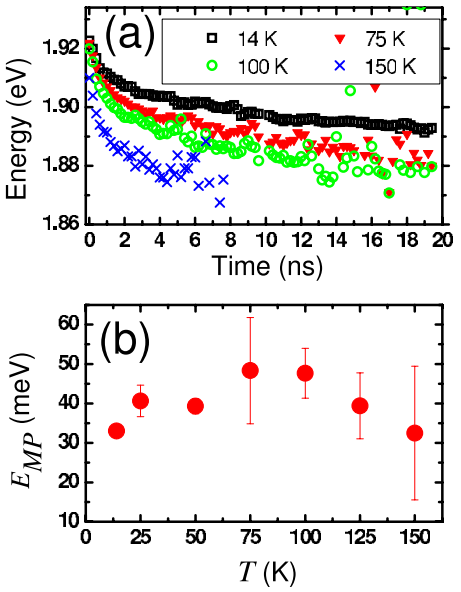

FIG. 6. (Color online) (a) Time dependence of the peak PL energy of sample 1 for temperatures ranging from 14 to 150 K. The overall energy displacement of the different curves reflects the thermal reduction in the band gap. (b) Temperature dependence of the magnetic-polaron formation energy (E_{MP}).

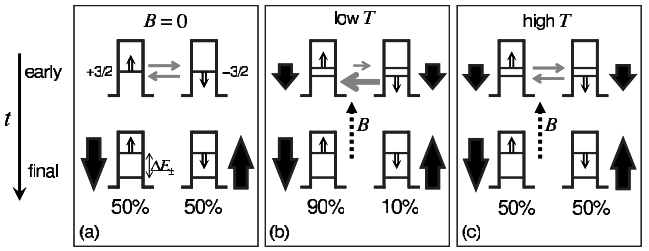

FIG. 7. Schematic illustrating magnetic-polaron formation in sample 1. (a) Zero magnetic field; (b) nonzero magnetic field B, low temperature T; and (c) nonzero B, high T. Double line arrows: hole spins; full arrows: z components of Mn spins; dotted arrows: applied magnetic field; and horizontal arrows: relative magnitudes of the hole spin-flip probabilities. Mn spin orientation is antiparallel to B. Top row: early times following excitation. Bottom row: final spin configuration. The numbers in the bottom row of (b) are an example of the percentage of QDs occupied by magnetic polarons with the hole spin parallel and antiparallel to the applied magnetic field; such a ratio would result in a high circular polarization of emission. The numbers in (c) correspond to zero polarization, found at high T.

tures; on average $\tau_1 \sim 0.7$ ns, and $\tau_2 \sim 11$ ns. We attribute τ_1 to the process of antiparallel alignment of the Mn spins with the spin of a hole. MP formation with two very different timescales has also been observed recently for colloidal QDs.[18] The slower process was attributed to directional reorientation of the MP due to crystal anisotropy. This mechanism is likely to be the origin of τ_2 in our QD because atomic force microscopy pictures from reference QD layers indicate strong shape anisotropy in the xy plane.

While our cw and TR PL measurements show the formation of MPs, there are important differences of their properties as compared with those in previous studies of magnetic QDs.[2,18] These differences are: the persistence of MPs at high temperatures and the weak T dependence of E_{MP}, as will be discussed below. Comparison of the PL peak energies in the cw and TR spectra reveals that the former correspond to fully formed MPs, which is consistent with $\tau_1 < \tau_{\mathrm{R}}$.[9] Thus, it may be surprising that the circular polarization P is practically zero at 80 K [see Fig. 2(a)], even though E_{MP} at 80 K is much larger than the corresponding thermal energy [see Fig. 6(b)], and the magnetic polaron itself persists up to 150 K. To explain this apparent paradox, we have developed a simple model for the formation of MP in our samples. Our model is related to an approach used to describe MPs in quantum wells.[31] The details of our model are illustrated in Fig. 7. In our analysis, we neglect the influence of electrons on the magneto-optical properties; since their exchange interaction as well as their wave function overlap with the Mn ions are much smaller than those of the holes [see Fig. 1(a)]. The preferred orientation of the hole spin is along the z axis due to the QD disk shape and the spin-orbit interaction.[32] The process of aligning the Mn spins via the h-Mn exchange interaction occurs on a time scale, which defines τ_{MP}. In Fig. 7(a) we show the h-Mn spin orientations at $B=0$. Upon photoexcitation of the holes, the average spin of the Mn ions is zero and therefore the two hole spin states ($\pm 3/2$) are degenerate. At later times, the spin of the hole aligns antiferromagnetically (AFM) with the Mn spins (in the same QD) via the h-Mn exchange interaction. The occupation of the spin-up ($+3/2$) hole state is the same as that of spin down ($-3/2$) leading to zero polarization of the emitted light. The redshift of the PL peak with time shown in Fig. 6(a) is due to the energy gained by the antiferromagnetic alignment of the hole and Mn spins. The energy difference $\Delta E_{\pm}$ between the ferromagnetic and antiferromagnetic h-Mn spin orientation is equal to twice the total redshift: $2E_{\mathrm{MP}} \gg 80$ meV. At intermediate times, the MP is forming, and $\Delta E_{\pm}$ is less than 80 meV. Electron-hole recombination occurs at intermediate times and stops the MP formation before it is fully developed. Photons associated with the recombination processes exhibit redshifts that are smaller than E_{MP}, as is shown in Fig. 6(a).

In Figs. 7(b) and 7(c) we discuss the magnetic polaron formation in the presence of an *external* magnetic field B at low ($T \sim 4.2$ K) and high ($T \sim 80$ K) temperatures, respectively. At short times after its photoexcitation, the hole occupies a spin-up or a spin-down level ($\pm 3/2$), with thermodynamic occupancy probabilities given by the initial spin splitting of hole levels. This splitting is caused by a small degree of Mn spin alignment, determined by the external magnetic field B and by T [see Figs. 7(b) and 7(c)].

At low temperatures, [Fig. 7(b)], the difference between the energies of the two possible initial h-Mn spin orientations is larger than the thermal energy $k_B T$. Thus, the higher energy state relaxes to the lower energy state via a spin flip of the hole with a higher probability than the opposite process. Both processes are indicated in the upper panel by the horizontal arrows, the size of which represents the hole spin-flip probability. As time progresses the magnetic polaron is formed; the two final h-Mn spin orientations as well as their possible occupation probabilities are shown in the lower panel of Fig. 7(b). The majority of the holes are in their

spin-up state and thus the net circular polarization of the emitted light is $\sigma+$ (recombination of $-1/2$ spin electrons with $+3/2$ spin holes). The larger size of (full) arrows in the lower panel of Fig. 7(b) indicates that the z component of the Mn spins increases due to the high effective magnetic field generated by the holes via the exchange interaction. These internal effective fields ($\sim$100 T) are an order of magnitude stronger that the externally applied field.[18]

In what follows, we discuss the magnetic polaron formation at high temperatures [Fig. 7(c)]. In the upper panel, we show the possible h-Mn spin orientations. The energy difference between the two states is smaller than the thermal energy k_BT, in contrast to the situation in Fig. 7(b). The hole spin-flip probabilities are now roughly equal as indicated by the sizes of the horizontal arrows. The redshifts in the lower panel of Fig. 7(c) are the same as those in the lower panel of Fig. 7(b) because in both cases they are mainly determined by the large internal effective magnetic field. Thus, at high temperatures, the MPs still form but the circular polarization of the emitted light is zero. This is because at elevated temperatures the population of spin up is the same as that of the spin-down holes and thus the intensities of the $\sigma+$ and $\sigma-$ interband transitions are equal to each other.

The measurements of E_{MP} as function of T in our QDs [Fig. 6(b)] reveal a very weak temperature dependence, which is discussed below. We interpret this behavior in terms of an anomalous T dependence of the magnetic susceptibility χ of the Mn spins in the QDs. To describe $\chi(T)$, we first note that the magnetic response of the QD system is most likely in the linear regime at 150 K. Since we find E_{MP} to be essentially temperature independent up to 150 K, we assume a linear response of the magnetization even at the lowest experimental temperatures. In this linear regime, as is the case for donor-bound MPs,[14] the two observable quantities E_{MP} and $\chi(T)$ are related to each other by the equation,

$$E_{\mathrm{MP}} = \mu_0^{-1}(J_{ex}/2g\mu_B N_0)^2 \eta(E_{\mathrm{MP}}/k_BT)\Omega_{eff}^{-1}\chi(T), \qquad (1)$$

where J_{ex} is the exchange integral for holes, N_0 is the cation density, $g=2$, μ_B is the Bohr magneton, and Ω_{eff} is the effective volume of the MP,[33] defined by $\Omega_{eff}^{-1}=\int|\psi(\mathbf{r})|^4 d\mathbf{r}$. Here ψ is the hole wave function. The term $\eta(E_{\mathrm{MP}}/k_BT)$ interpolates between the two limiting cases of strong, $\eta(x)=\tanh(x)$, and weak, $\eta(x)=\tanh x+2/x$, magnetic anisotropies.[14] The former case is essentially the Ising model of a MP.[15] The latter case corresponds to fully isotropic spin fluctuations[14] and can be applied to spherically shaped QDs in the limit of vanishing spin-orbit interaction.

First we use Eq. (1) to investigate the magnitude of E_{MP} at low T (where $\eta=1$ for both models). The very small PL peak shift with B shown in Fig. 2(b) indicates an exceptionally low χ. We attribute the low susceptibility to a combination of AFM Mn coupling and shape anisotropy of the QDs, which have the form of disks with height much smaller than the disk diameter. The strong AFM character of the Mn-Mn interaction is manifested in the properties of bulk[34] and epitaxial[35] MnTe. Since Mn acts as a nucleation center for the growth of QDs in migration-enhanced epitaxy, its local concentration in the dots could be considerably higher than the average value of 5.2%,[36] and is expected to result in more pronounced AFM behavior.

The low susceptibility in this system must be compensated by a small Ω_{eff} (strong confinement) to obtain the large E_{MP} observed in our experiments. We model the confinement of the disk-shaped QDs by a widely used form:[37] a parabolic potential in the x-y plane and an infinite rectangular potential along z axis. We find for the ground state: $\Omega_{eff}=\pi\hbar(m^*E_b/2)^{-1/2}dh/3$, where E_b is the (Zn,Mn)Te/ZnSe valence-band offset while d and h are the disk's diameter and height, respectively. With $E_b=1$ eV,[38] $d=20$ nm, $h=3$ nm, and $m^*=0.19m_0$,[39] this expression gives a MP effective volume Ω_{eff} an order of magnitude smaller than the QD volume. Further reduction in Ω_{eff} may result from additional hole localization during MP formation. Similar strong hole localization effects were also found in type-II magnetic quantum wells.[17] The value of E_{MP} measured in our experiments is almost three times larger than the value in Ref. 2, even though the p-d exchange integrals in (Zn,Mn)Te ($J_{ex}=1.05$ eV) and (Zn,Mn)Se ($J_{ex}=1.11$ eV) are very similar.[1] We attribute this difference to the fact that the Mn and the holes are both located in the (Zn,Mn)Te QDs, which leads to an enhancement of the h-Mn exchange interaction. In contrast, in the samples of Ref. 2, the holes were confined in the CdSe QDs and the Mn ions were located in the surrounding (Zn,Mn)Se matrix.

Next, from the E_{MP} versus T plot of Fig. 6(b), we conclude that E_{MP} is approximately temperature independent. If there is a temperature variation in E_{MP}, it is small. The relatively large error bars for $E_{\mathrm{MP}}(T)$ at higher temperatures in Fig. 6(b) result from our use of very small excitation powers (200 μW) to avoid possible band bending (dipole layer formation). The average value of E_{MP} is 40 meV.

To consider the case, in which the hole g factor anisotropy as well as the QD shape anisotropy vanish, we substitute E_{MP} into Eq. (1) and calculate $\chi(T)$. The results are plotted in Fig. 8 using squares. The system seems to behave like a "paramagnet" with an unreastically high AFM temperature T_{AF}.[39] The temperature decrease in χ is much weaker than for conventional type-I magnetic QDs, as extrapolated from the low-T behavior of $E_{\mathrm{MP}}(T)$ given in Ref. 2.

The fully isotropic case discussed above is not realistic, but it is important to consider it, as it provides a lower bound for $\chi(T)$. Our system is much closer to the high anisotropy case described by the equation $\eta(x)=\tanh(x)$, with the easy magnetization axis for the Mn lying in the xy plane, and we consider it as the second possibility. Two anisotropies must be taken into account: (1) that of the magnetic susceptibility, $\chi_z \neq \chi_{xy}$, where χ_z (χ_{xy}) is the susceptibility along the z axis (in the xy plane) and (2) that of the heavy hole g factor, i.e., $g_z \gg g_{xy}$, due to strong spin-orbit coupling and a quasi-two-dimensional shape of the hole wave function.[32] The g factor anisotropy causes the system to behave as an Ising-type MP, with temperature dependence following that of χ_z, Fig. 8 circles.

Below we propose a model based on the Ising-type MPs that describes our results: in the absence of holes the Mn spins in the QDs lie in the xy plane, and are coupled antiferromagnetically[1] as shown in Fig. 9(a). Following photoexcitation, the photogenerated spin $\pm 3/2$ holes form MPs

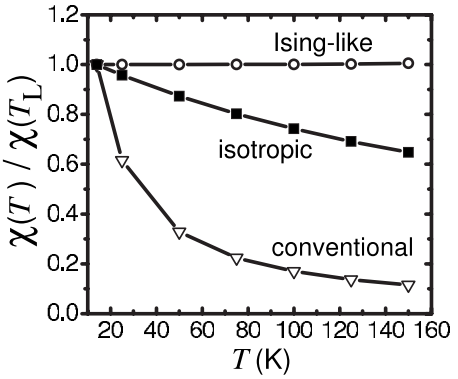

FIG. 8. Temperature dependence of magnetic susceptibility χ determined from $E_{MP}(T)$ shown in Fig. 6(b) for different QD models: squares: fully isotropic QDs and circles: highly anisotropic QDs, i.e., Ising-type system. The conventional susceptibility of magnetic QDs (Ref. 2) is shown with triangles. All χ's are normalized to their values at the lowest experimental temperature, $T_L = 14$ K.

with the Mn as follows: exchange coupling between the hole and Mn spins results in canting of the Mn spins, which acquire a small z component as shown in Fig. 9(b) for both hole spin orientations. In each case, the hole and Mn spins are coupled antiferromagnetically and reduce the energy of the h-Mn complex. Thus, we have a unique magnetic ordering with the Mn spins locked antiferromagnetically in xy plane, and partially aligned along the z axis following the formation of the magnetic polaron. The overall weak temperature dependence of MP in our work is consistent with the fact that the transverse susceptibility (χ_z) of antiferromagnets depends weakly on T.[40] The small value of the exciton Zeeman splitting implies that χ_z has a correspondingly small value. The low susceptibility is compatible with the relatively long spin alignment time, $\tau_1 \sim 700$ ps observed in our work, as compared to $\tau_{MP} < 200$ ps reported in Ref. 2. Similar models that describe MP polaron formation based on canting of the Mn spins, which arises from the h-Mn exchange interaction, were suggested for bulk (In,Mn)As and for (III,Mn)V-based QWs.[41,42]

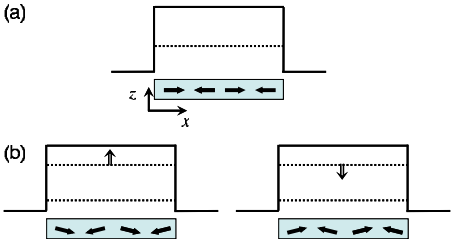

FIG. 9. (Color online) Schematic of the Mn-hole spin alignment based on our results. Double arrows: hole spins and full arrows: Mn spins. (a) Prior to hole photoexcitation; Mn spins are coupled antiferromagnetically and lie in the x-y plane. (b) Following the hole photoexcitation and MP formation. Two MP states are possible that correspond to the two hole spin states. In the absence of an applied magnetic field, these two states are equally probable [see Fig. 7(a)].

IV. CONCLUSIONS

In this paper, we describe the results of a magneto-optical study of (Zn,Mn)Te/ZnSe type-II quantum dots that show the formation of exciton magnetic polarons. This system has the following characteristics: (a) strong circular polarization of the type-II exciton emission at low temperature that decreases sharply with increasing temperature and disappears above 80 K; (b) small exciton Zeeman splitting as measured by cw PL; and (c) large redshift of the exciton energy as function of time in time-resolved PL. The total redshift, which we identify as the magnetic polaron formation energy, is roughly independent of temperature and persists up to 150 K. These seemingly contradictory properties are interpreted in terms of a model, which takes into account the hole-Mn as well as the Mn-Mn exchange coupling and their role in the magnetic polaron formation.

We expect that our findings will stimulate further experimental studies of type-II magnetic QDs in order to better understand the properties of this unique system, which could find applications in spin-based devices.

ACKNOWLEDGMENTS

This work was supported by NSF under Grant No. ECCS0824220, ONR under Grant No. N000140910113, DOE-BES, NSF-ECCS Career, US ONR under Grant No. N000140610123, and AFOSR-DCT.

*ian.sellers@sharp.co.uk
†Present address: Sharp Laboratories of Europe Ltd., Oxford Science Park, Oxford OX4 4GB, UK.
‡rmo@buffalo.edu

[1] J. K. Furdyna, J. Appl. Phys. **64**, R29 (1988).
[2] J. Seufert, G. Bacher, M. Scheibner, A. Forchel, S. Lee, M. Dobrowolska, and J. K. Furdyna, Phys. Rev. Lett. **88**, 027402 (2001).
[3] S. Mackowski, T. Gurung, T. A. Nguyen, H. E. Jackson, L. M. Smith, G. Karczewski, and J. Kossut, Appl. Phys. Lett. **84**, 3337 (2004).
[4] Y. Léger, L. Besombes, J. Fernández-Rossier, L. Maingault, and H. Mariette, Phys. Rev. Lett. **97**, 107401 (2006).
[5] C. Gould, A. Slobodskyy, D. Supp, T. Slobodskyy, P. Grabs, P. Hawrylak, F. Qu, G. Schmidt, and L. W. Molenkamp, Phys. Rev. Lett. **97**, 017202 (2006).
[6] Y. Léger, L. Besombes, L. Maingault, D. Ferrand, and H. Mariette, Phys. Rev. Lett. **95**, 047403 (2005).
[7] R. Beaulac, P. I. Archer, S. T. Ochsenbein, and D. R. Gamelin, Adv. Funct. Mater. **18**, 3873 (2008).
[8] I. Žutić, J. Fabian, and S. Das Sarma, Rev. Mod. Phys. **76**, 323 (2004).

[9] G. Mackh, W. Ossau, D. R. Yakovlev, A. Waag, G. Landwehr, R. Hellmann, and E. O. Gobel, Phys. Rev. B **49**, 10248 (1994).
[10] J. Fernández-Rossier and L. Brey, Phys. Rev. Lett. **93**, 117201 (2004).
[11] A. O. Govorov, Phys. Rev. B **72**, 075359 (2005).
[12] R. M. Abolfath, P. Hawrylak, and I. Zutic, Phys. Rev. Lett. **98**, 207203 (2007).
[13] R. M. Abolfath, A. G. Petukhov, and I. Zutic, Phys. Rev. Lett. **101**, 207202 (2008).
[14] T. Dietl and J. Spalek, Phys. Rev. Lett. **48**, 355 (1982).
[15] P. A. Wolff, Semicond. Semimetals **25**, 413 (1988).
[16] D. Heiman, P. A. Wolff, and J. Warnock, Phys. Rev. B **27**, 4848 (1983).
[17] A. A. Toropov, Y. V. Terent'ev, S. V. Sorokin, S. V. Ivanov, T. Koyama, K. Nishibayashi, A. Murayama, Y. Oka, J. P. Bergman, I. A. Buyanova, W. M. Chen, and B. Monemar, Phys. Rev. B **73**, 245335 (2006).
[18] R. Beaulac, L. Schneider, P. I. Archer, G. Bacher, and D. R. Gamelin, Science **325**, 973 (2009).
[19] I. L. Kuskovsky, W. MacDonald, A. O. Govorov, L. Muroukh, X. Wei, M. C. Tamargo, M. Tadic, and F. M. Peeters, Phys. Rev. B **76**, 035342 (2007).
[20] I. R. Sellers, V. R. Whiteside, A. O. Govorov, W. C. Fan, W. C. Chou, I. Khan, A. Petrou, and B. D. McCombe, Phys. Rev. B **77**, 241302 (2008).
[21] M. C. K. Cheung, A. N. Cartwright, I. R. Sellers, B. D. McCombe, and I. L. Kuskovsky, Appl. Phys. Lett. **92**, 032106 (2008).
[22] X. Zhou, M. Muñoz, S. Guo, M. C. Tamargo, Y. Gu, I. L. Kuskovsky, and G. F Neumark, J. Vac. Sci. Technol. B **22**, 1518 (2004).
[23] F. Gindele, U. Woggon, W. Langbein, J. M. Hvam, K. Leonardi, D. Hommel, and H. Selke, Phys. Rev. B **60**, 8773 (1999).
[24] M. C. Kuo, J. S. Hsu, J. L. Shen, K. C. Chiu, W. C. Fan, Y. C. Lin, C. H. Chia, W. C. Chou, M. Yasar, R. Mallory, A. Petrou, and H. Luo, Appl. Phys. Lett. **89**, 263111 (2006).
[25] G. Barilero, C. Rigaux, M. Menant, Nguyen Hy Hau, and W. Giriat, Phys. Rev. B **32**, 5144 (1985).
[26] P. Wojnar, J. Suffczynski, A. Golnik, A. Ebbens, U. Woggon, G. Karczewski, and J. Kossut, Phys. Rev. B **80**, 195321 (2009).
[27] G. Bacher, A. A. Maksimov, H. Schömig, V. D. Kulakovskii, M. K. Welsch, A. Forchel, P. S. Dorozhkin, A. V. Chernenko, S. Lee, M. Dobrowolska, and J. K. Furdyna, Phys. Rev. Lett. **89**, 127201 (2002).
[28] Y. Gu, I. L. Kuskovsky, M. van der Voort, G. F. Neumark, X. Zhou, and M. C. Tamargo, Phys. Rev. B **71**, 045340 (2005).
[29] D. R. Yakovlev and K. V. Kavokin, Comments Condens. Matter Phys. **18**, 51 (1996).
[30] J. J. Zayhowski, R. N. Kershaw, D. Ridgley, K. Dwight, A. Wold, R. R. Galazka, and W. Giriat, Phys. Rev. B **35**, 6950 (1987).
[31] V. P. Kochereshko, I. A. Merkulov, G. R. Pozina, I. N. Uraltsev, D. R. Yakovlev, W. Ossau, A. Waag, and G. Landwehr, Solid-State Electron. **37**, 1081 (1994).
[32] P. S. Dorozhkin, A. V. Chernenko, V. D. Kulakovskii, A. S. Brichkin, A. A. Maksimov, H. Schoemig, G. Bacher, A. Forchel, S. Lee, M. Dobrowolska, and J. K. Furdyna, Phys. Rev. B **68**, 195313 (2003).
[33] K. V. Kavokin, I. A. Merkulov, D. R. Yakovlev, W. Ossau, and G. Landwehr, Phys. Rev. B **60**, 16499 (1999).
[34] K. Walther, Solid State Commun. **5**, 399 (1967).
[35] P. Kłosowski, T. M. Giebułtowicz, J. J. Rhyne, N. Samarth, H. Luo, and J. K. Furdyna, J. Appl. Phys. **70**, 6221 (1991).
[36] A. P. Li, C. Zeng, K. van Benthem, M. F. Chisholm, J. Shen, S. V. S. Nageswara Rao, S. K. Dixit, L. C. Feldman, A. G. Petukhov, M. Foygel, and H. H. Weitering, Phys. Rev. B **75**, 201201 (2007).
[37] L. Jacak, P. Hawrylak, and A. Wójs, *Quantum Dots* (Springer, Berlin, New York, 1998).
[38] C. S. Yang, Y. J. Lai, W. C. Chou, W. K. Chen, M. C. Lee, M. C. Kuo, J. Lee, J. L. Shen, D. J. Jang, and Y. C. Cheng, J. Appl. Phys. **97**, 033514 (2005).
[39] D. Ferrand, J. Cibert, A. Wasiela, C. Bourgognon, S. Tatarenko, G. Fishman, T. Andrearczyk, J. Jaroszyński, S. Koleśnik, T. Dietl, B. Barbara, and D. Dufeu, Phys. Rev. B **63**, 085201 (2001).
[40] N. W. Ashcroft and N. D. Mermin, *Solid State Physics* (Holt, New York, 1976).
[41] H. Ohno, H. Munekata, T. Penney, S. von Molnar, and L. L. Chang, Phys. Rev. Lett. **68**, 2664 (1992).
[42] Y. G. Semenov and K. W. Kim, Phys. Rev. B **70**, 125303 (2004).